Target Localization Accuracy and Multiple Target Localization: Tradeoff in MIMO Radars

Hana Godrich°, Alexander M. Haimovich°, and Rick S. Blum†
°New Jersey Institute of Technology, Newark, NJ 07102, email: [hg44,haimovich]@njit.edu
†Lehigh University, Bethlehem, PA 18015-3084, email: rblum@eecs.lehigh.edu

***Abstract*— This paper undertakes the study of localization performance of multiple targets in coherent MIMO radar systems with widely spread elements. MIMO radar systems with coherent processing and a single target were shown to benefit from a coherency and spatial advantages. The first is proportional to the ratio of the signal carrier frequency to the effective bandwidth, while the latter provides a gain proportional to the product of the number of transmitting and receiving sensors. In the current study, the model in extended to the estimation accuracy of multiple targets. The Cramer-Rao lower bound (CRLB) for the multiple targets localization problem is derived and analyzed. The localization is shown to benefit from coherency advantage. The tradeoff between target localization accuracy and the number of targets that can be localized is shown to be incorporated in the spatial advantage term. An increase in the number of targets to be localized exposes the system to increased mutual interferences. This tradeoff depends on the geometric footprint of both the sensors and the targets, and the relative positions of the two. Numerical analysis of some special cases offers an insight to the mutual relation between a given deployment of radars and targets and the spatial advantage it presents.**

***Index Terms*— MIMO radars, CRLB, target localization.**

I. Introduction

MIMO radar is a rapidly expanding research field [1]-[13]. These systems have the ability to transmit diverse waveforms ranging from independent to fully correlated [7]. MIMO radar architectures may be generally classified into colocated antenna schemes or widely distributed over a given area. For colocated antennas, waveform diversity [4] is being exploited, while distributed antenna takes advantage of the spatial diversity supported by the system configuration [1]. As each configuration and model has its strengths and challenges, it is already apparent that they have the potential to make important contributions to the radar field.

Enhanced target parameter estimation capabilities is one of MIMO radar systems attributes. Specifically, its ability to separate multiple targets [9], [10], and estimate targets' parameters such as direction-of-arrival (DOA) [4], [5], and range [11]–[13].

MIMO radar system with colocated antenna perform DOA estimation of targets in the far-field. In this class of systems, extensive research [7], [8], [10] has focused on waveform design and optimization targeted at reducing the cross-correlation of the signals reflected from various targets to improve bearing separation in multiple targets scenarios. Some of the waveform optimization techniques suggested in [6] are based on the Cramer-Rao lower bound (CRLB) matrix [15].

Evaluation of single target localization accuracy performance for coherent MIMO radar systems with widely distributed antenna is provided in [13]. It is shown, utilizing the CRLB, that a coherency advantage, proportional to the ratio between the signal carrier frequency and the signal effective bandwidth, is achieved. In addition, a spatial advantage of the order of the product of the number of transmit and receive radars is generated. In this paper, the study is extended to the case of multiple targets, dealing with the possible tradeoffs that the increased number of targets imposes on the localization accuracy performances. The CRLB is derived and evaluated for this case. Coherency and spatial advantages are identified and analyzed. As the spatial advantage is strongly reliant on the geographical setting of the radars with respect to the targets and on the geometric distribution of targets, an insight into the system inherent tradeoffs is provided using numerical analysis.

The paper is organized as follows: the system signal model is introduced in Section II. In Section III the CRLB on the targets localization estimation errors is derived. Tradeoffs between performance and the number of targets is presented by numerical analysis in Section IV. Finally, Section V concludes the paper.

II. System Model

Assume M transmitting radars and N receiving radars, widely distributed and time and phase synchronized. The receiving radars could be colocated with the transmitting ones or widely separated. The transmitting and receiving radars are located in a two dimensional plane (x, y). Consider Q point targets located at coordinates $X_q = (x_q, y_q)$, $q = 1, ..., Q$. A set of orthogonal waveforms is transmitted, with the lowpass equivalent $s_k(t)$, $k = 1, \ldots, M$. The power of the transmitted waveforms is normalized such that the aggregate power transmitted by the sensors is constant, irrespective of the number of transmit sensors. Let all transmitted waveforms be narrowband signals with individual effective bandwidth β_k defined as $\beta_k^2 = \int_{W_k} f^2 |S_k(f)|^2 df / \int_{W_k} |S_k(f)|^2 df$, where the integration is over the range of frequencies with non-zero signal content W_k [16]. The signals are narrowband in the sense that for a carrier frequency of f_c, the narrowband signal assumption implies $\beta_k^2 / f_c^2 \ll 1$. Assume the Q targets are

A. M. Haimovich work was supported by the U.S. Air Force Office of Scientific Research, Agreement FA9550-06-1-0026. R. S. Blum work was supported by the Air Force Research Laboratory under agreement No. FA9550-06-1-0041

located within a search cell of c/β, where $\beta = \max\{\beta_k\}$. The targets are modeled as point scatterers with complex amplitude $\zeta^q = \zeta^q_{re} + j\zeta^q_{im}$. To simplify the notation, the signal power term is embedded in the noise variance term such that the signal-to-noise ratio (SNR) at the transmitter, denoted SNR, and is defined as the transmitted power by a sensor divided by the noise power at a receiving sensor. The following notations are introduced for later use: $\tau^q_{\ell k} = \tau_{\ell k}(X_q)$, $\tau^q = [\tau^q_{11}, ..., \tau^q_{MN}]$, and $\zeta^q = [\zeta^q_{re}, \zeta^q_{im}]$.

In the model developed below, path loss effects are neglected, i.e., the model accounts for the effect of the sensors/targets locations only through time delays (or phase shifts) of the signals. For convenience, we define a $4Q$ dimensioned vector θ of the unknown parameters:

$$\theta \stackrel{\text{def}}{=} \left[x_1, y_1, ..., x_Q, y_Q, \zeta^1, ..., \zeta^Q\right]^T. \tag{1}$$

The propagation time estimate of a signal transmitted by the k-th transmitting radar located at coordinates $T_k = (x_{tk}, y_{tk})$,reflected by a target located at X_q, and received by a sensor located at $R_\ell = (x_{r\ell}, y_{r\ell})$, can be expressed as:

$$\widehat{\tau}^q_{\ell k} = \tau^q_{\ell k} + \varepsilon^q_{\ell k}, \tag{2}$$

where $k = 1, .., M$, $\ell = 1, .., N$, $q = 1, .., Q$ and $\tau^q_{\ell k}$, the propagation time, is the sum of the time delays from radar k to target q and from the target to radar ℓ:

$$\tau^q_{\ell k} = \frac{1}{c}\left(\sqrt{(x_{tk} - x^q)^2 + (y_{tk} - y^q)^2} + \sqrt{(x_{r\ell} - x^q)^2 + (y_{r\ell} - y^q)^2}\right), \tag{3}$$

and $\varepsilon^q_{\ell k}$ is the estimation error. The speed of light is denoted by c.

Consider the case of a baseband representation of the signal observed at sensor ℓ due to a transmission from sensor k and reflection from Q scatterers, given by:

$$r_\ell(t) = \sum_{q=1}^{Q}\sum_{k=1}^{M}\zeta^q s_k\left(t - \tau^q_{\ell k}\right)\rho^q_{\ell k} + w_\ell(t), \tag{4}$$

where $\rho^q_{\ell k} = \exp\left(-j2\pi f_c \tau^q_{\ell k}\right)$ accounts for the phase shift due to the propagation delay. Others terms are the carrier frequency f_c, circularly symmetric, zero-mean, complex Gaussian noise $w_\ell(t)$, which is spatially and temporally white with autocorrelation function $\sigma^2_w \delta(\tau)$. We define the vectors $\mathbf{r} = [r_1(t), \ldots, r_N(t)]^T$ and $\psi = \left[\tau^1, ..., \tau^Q, \zeta^1, .., \zeta^Q\right]^T$ for later use. The received signal at each sensor is a mixture of the transmitted signals reflected by the targets. The mixture of signals is separated at the receiver end by exploiting the orthogonality between the transmitted waveforms.

III. The CRLB on Targets Location Estimation

The CRLB provides a lower bound for the mean square error (MSE) of any unbiased estimator for an unknown parameter(s). Given a vector parameter θ, and the conditional joint probability density function (pdf) of $\mathbf{r}$ given θ, $p(\mathbf{r}|\theta)$, the unbiased estimate $\widehat{\theta}$ satisfies the following inequality [15]:

$$E_\theta\left\{\left(\widehat{\theta}_i - \theta_i\right)\left(\widehat{\theta}_i - \theta_i\right)^T\right\} \geq \left[\mathbf{J}^{-1}(\theta)\right]_{i,i}, \tag{5}$$

where $\mathbf{J}(\theta)$ is the Fisher Information matrix (FIM) given by:

$$\mathbf{J}(\theta) \stackrel{\text{def}}{=} E_\theta\left\{\frac{\partial}{\partial\theta}\log p(\mathbf{r}|\theta)\left(\frac{\partial}{\partial\theta}\log p(\mathbf{r}|\theta)\right)^H\right\}. \tag{6}$$

Let the CRLB matrix be defined as:

$$\mathbf{C}_{CRLB} = \left[\mathbf{J}(\theta)\right]^{-1}. \tag{7}$$

Since the received signal in (4) is defined as a function of the time of arrival, $\tau^q_{\ell k}$, and the reflectivity value ζ^q, with the use of the *chain rule*, $\mathbf{J}(\theta)$ could be decomposed into the alternative form [15]:

$$\mathbf{J}(\theta) = \begin{bmatrix} \mathbf{D} & \mathbf{0} \\ \mathbf{0} & \mathbf{I}_{2Q\times 2Q} \end{bmatrix} \mathbf{J}(\psi) \begin{bmatrix} \mathbf{D} & \mathbf{0} \\ \mathbf{0} & \mathbf{I}_{2Q\times 2Q} \end{bmatrix}^T, \tag{8}$$

where ψ was defined earlier, and $\mathbf{J}(\psi)$ is the FIM for the unknown vector ψ. In order to derive the FIM given in (8), the joint pdf $p(\mathbf{r}|\psi)$ is required. Given the signal model (4) and the set of known waveforms $s_k\left(t - \tau^q_{\ell k}\right)$ parameterized by the unknown time delays $\tau^q_{\ell k}$, the joint pdf of the observations parameterized by the unknown parameters vector ψ, is:

$$p(\mathbf{r}|\psi) \propto \exp \left\{-\frac{1}{\sigma^2_w}\sum_{\ell=1}^{N}\int_T \left|r_\ell(t) - \sum_{q=1}^{Q}\sum_{k=1}^{M}\zeta^q s_k\left(t - \tau^q_{\ell k}\right)\rho^q_{\ell k}\right|^2 dt\right\}. \tag{9}$$

The matrix $\mathbf{D}$ is of the form:

$$\mathbf{D} = -\frac{1}{c}\begin{bmatrix} \mathbf{D}^1 & \cdots & \mathbf{0}_{2\times MN} \\ \vdots & \ddots & \vdots \\ \mathbf{0}_{2\times MN} & \cdots & \mathbf{D}^Q \end{bmatrix}_{2Q\times MNQ}, \tag{10}$$

where submatrix $\mathbf{D}^q$ is derived as:

$$\mathbf{D}^q = \begin{bmatrix} \frac{\partial\tau^q_{11}}{\partial x^q} & \cdots & \frac{\partial\tau^q_{MN}}{\partial x^q} \\ \frac{\partial\tau^q_{11}}{\partial y^q} & \cdots & \frac{\partial\tau^q_{MN}}{\partial y^q} \end{bmatrix}_{2\times MN}. \tag{11}$$

Using (3) in (11), matrix $\mathbf{D}^q$ is calculated as:

$$\mathbf{D}^q = \begin{bmatrix} \cos\phi^q_1 + \cos\varphi^q_1 & \ldots & \cos\phi^q_M + \cos\varphi^q_N \\ \sin\phi^q_1 + \sin\varphi^q_1 & \ldots & \sin\phi^q_M + \sin\varphi^q_N \end{bmatrix}, \tag{12}$$

where the phase $\phi^q_k = \tan^{-1}\left(\frac{y^q - y_{tk}}{x^q - x_{tk}}\right)$ is the bearing angle of the transmitting sensor k to target q measured with respect to the x axis; the phase $\varphi^q_\ell = \tan^{-1}\left(\frac{y^q - y_{r\ell}}{x^q - x_{r\ell}}\right)$ is the bearing angle of the receiving radar ℓ to target q measured with respect to the x axis. Thus, matrix $\mathbf{D}^q$ includes the geometric information of the radars' location configuration relative to the position of the qth target.

An expression for the FIM $\mathbf{J}(\psi)$, is derived in Appendix I, yielding:

$$\mathbf{J}(\psi) = \eta_o \begin{bmatrix} \mathbf{\Gamma} & \mathbf{V}^T \\ \mathbf{V} & \mathbf{\Sigma}_\zeta \end{bmatrix}_{(2+MN)Q\times(2+MN)Q}, \quad (13)$$

with $\eta_o = 8\pi^2 \,\mathrm{SNR}\, f_c^2$ and the block matrices $\mathbf{\Gamma}$, $\mathbf{\Sigma}_\zeta$, and $\mathbf{V}$ are defined in Appendix I in (23), (26), and (29), respectively.

In order to determine the value of $\mathbf{J}(\theta)$, we use (13) and (10) in (8), to obtain the following FIM matrix:

$$\mathbf{J}(\theta) = \frac{8\pi^2 \,\mathrm{SNR}\, f_c^2}{c^2} \begin{bmatrix} \mathbf{D\Gamma D}^T & \mathbf{DV}^T \\ \mathbf{VD}^T & \mathbf{\Sigma}_\zeta \end{bmatrix}_{4Q\times 4Q}. \quad (14)$$

While the CRLB expresses the lower bound on the variance of the estimate of $\theta = \left[x_1, y_1, ..., x_Q, y_Q, \zeta^1, ..., \zeta^Q\right]^T$, we are really interested in the estimation of only the targets locations $(x_1, y_1, ..., x_Q, y_Q)$. For the variances of the estimates of x_q and y_q, it is sufficient to derive the $2Q \times 2Q$ upper left submatrix $[\mathbf{C}_{CRLB}]_{2Q\times 2Q} = [\mathbf{J}(\theta)]^{-1}_{2Q\times 2Q}$, which can be expressed [12]:

$$[\mathbf{C}_{CRLB}]_{2Q\times 2Q} = \eta(f_c)\left(\mathbf{D\Gamma D}^T - \mathbf{VD}^T\mathbf{\Sigma}_\zeta^{-1}\mathbf{DV}^T\right)^{-1}, \quad (15)$$

where $\eta(f_c) = \frac{c^2}{8\pi^2 \,\mathrm{SNR}\, f_c^2}$. The diagonal elements of the submatrix $[\mathbf{C}_{CRLB}]_{2Q\times 2Q}$ provide the lower bound on the localization mean squared error (MSE), $\sigma^2_{x_q} \geq \sigma^2_{CRx_q} = [\mathbf{C}_{CRLB}]_{2q-1,2q-1}$ and $\sigma^2_{y_q} \geq \sigma^2_{CRy_q} = [\mathbf{C}_{CRLB}]_{2q,2q}$, where these terms may be defined as:

$$\sigma^2_{CRx_q} = \eta(f_c)\cdot\eta_{Spt}(x_q) \quad (16)$$

$$\sigma^2_{CRy_q} = \eta(f_c)\cdot\eta_{Spt}(y_q), \quad (17)$$

and

$$\eta_{Spt}(x_q) = \left[\left(\mathbf{D\Gamma_x D}^T - \mathbf{VD}^T\mathbf{\Sigma}_\zeta^{-1}\mathbf{DV}^T\right)^{-1}\right]_{2q-1,2q-1} \quad (18)$$

$$\eta_{Spt}(y_q) = \left[\left(\mathbf{D\Gamma_x D}^T - \mathbf{VD}^T\mathbf{\Sigma}_\zeta^{-1}\mathbf{DV}^T\right)^{-1}\right]_{2q,2q}, \quad (19)$$

The CRLB matrix is related to the sensors and targets locations through matrices $\mathbf{D}$, $\mathbf{\Gamma_x}$ and $\mathbf{V}$, while the latter two are also functions of the received waveforms correlation functions and its derivatives. This dependency is captured in the terms $\eta_{Spt}(x_q)$ and $\eta_{Spt}(y_q)$, where further analysis is required.

A. Discussion

The expression for the CRLB as given in (15), provides insight into the performance of multiple targets localization accuracy performance of MIMO radars systems with coherent processing.

1) Coherency advantage: As in the single target case, the lower bound on the targets localization errors is inversely proportional to the carrier frequency f_c and independent of the signal individual effective bandwidth, due to the use of the phase information across the different paths. It is apparent that coherent processing offers a target localization precision gain of the order of f_c/β, referred to as *coherency advantage*.

The improvement in localization accuracy needs to be moderated with the observation that the CRLB is a bound of *small errors*. As such, it ignores effects that could lead to *large errors*. For example, MIMO radar with distributed sensors and coherent observations is subject to high sidelobes [2], [14]. Additionally, a phase coherent system is sensitive to phase errors. These topics are outside the scope of this paper, but they should be kept in perspective.

2) Spatial advantage: The CRLB submatrix terms are strongly reliant on the relative geographical spread of the radar sensors versus the targets locations. In MIMO radar, the targets play a similar role to the transmission channel in MIMO communication. As such, the elements in the CRLB, $\mathbf{\Gamma}_\mathbf{x}^{qq'}$ and $\mathbf{V}^{qq'}, q \neq q\prime$ may be viewed as overlapping multipath arrivals for a given ℓk propagation path. The trace of the CRLB provides an averaged spatial term $\eta_{Spt} = \frac{1}{Q}\sum_{q=1}^{Q}\left(\eta_{Spt}(x_q) + \eta_{Spt}(y_q)\right)$, and may be written as:

$$\eta_{Spt} = \mathrm{tr}\left\{\begin{array}{c} \sum_{q=1}^{Q}\Big[\mathbf{D}^q\mathbf{\Gamma}^{qq}\mathbf{D}^{q^T} - \mathbf{V}^{qq}\mathbf{D}^{q^T}\mathbf{\Psi}^{qq}\mathbf{D}^q\mathbf{V}^{qq^T} \\ - \sum_{q'\neq q=1}^{Q}\mathbf{V}^{qq'}\mathbf{D}^{q'^T}\mathbf{\Psi}^{q'q}\mathbf{D}^q\mathbf{V}^{qq'^T}\Big] \end{array}\right\}^{-1} \quad (20)$$

where $\mathbf{\Psi}^{q'q} = \mathbf{\Sigma}_\zeta^{-1}$. The first two terms in (20) are the auto-correlation terms, while the third term represents the cross-correlation between targets and therefore, serves as mutual interference. The elements of these cross-correlation matrices are products of the phase and amplitude elements, $\exp\left(-2\pi f_c \Delta\tau_{\ell k}^{qq'}\right)$ and $\int s_k\left(t - \Delta\tau_{\ell k}^{qq'}\right)s_k^*(t)\,dt$, where $\Delta\tau_{\ell k}^{qq'} = \tau_{\ell k}^{q} - \tau_{\ell k}^{q'}$, and its derivatives (see (23) and (29) in the appendix). As the distance between the targets impacts the time delay differences, $\Delta\tau_{\ell k}^{qq'}$, the following might be gleaned by inspection of (20):

- Targets separated by distances larger than a c/β resolution cell are resolvable with negligible loss in performance relative to the single target case. This results from the decorrelation achieved by this scenario, where the third term in (20) approaches zero. On the other end, distances smaller than the carrier wavelength λ are non-resolvable.
- The interference on paths ℓk for target q add in-phase with $\frac{c\Delta\tau_{\ell k}^{qq'}}{\lambda} \approx u$, $u = 0, 1, 2, ...$, i.e. $\cos\left(-2\pi f_c\Delta\tau_{\ell k}^{qq'}\right) \simeq 1$. They add out-of-phase with $\frac{c\Delta\tau_{\ell k}^{qq'}}{4\lambda} \approx u$, $u = 1, 2, ...$, i.e. $\cos\left(-2\pi f_c\Delta\tau_{\ell k}^{qq'}\right) \ll 1$. It is evident that the number of resolvable paths varies with the position of the radars with respect to the targets and the targets layout, where some may be

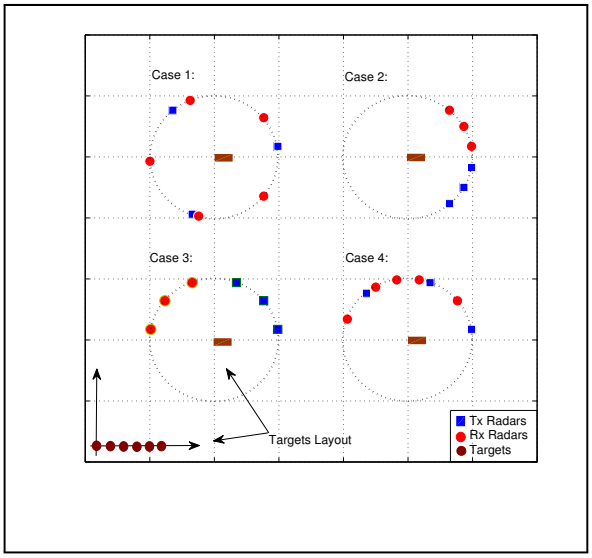

Fig. 1. System layout for cases 1 to 4.

more favorable than others. The number of resolvable propagation paths per target q and the geometric merit of these paths (integrated in matrix $\mathbf{D}^q$) determines the ability to localize target q and the localization accuracy quality. A minimum of 3 resolvable paths is required for the localization of a single target.

- Transmit and receive radar pairs, ℓk, with large aperture with respect to the targets layout are preferable due to the larger time delay differences they offer.
- Sensors placement needs to take into account the vertical and horizontal plane sensitivity needed for a given targets layout. For example, a horizontal targets layout requires better horizontal separation, achieved by broadside horizontal radar geometry.

To get a more intuitive understanding of the reliance of the spatial advantage on the geographical spread of the radars and targets, numerical analysis is employed in the next section for some special cases.

IV. Numerical Analysis

As mentioned previously, we show in [13] that the spatial advantage for the case of a single target is $MN/2$ under optimal conditions, i.e. when the target is located at the center of a virtual circle created by uniformly spaced sensors. In the case of multiple targets, the spatial advantage relies on the number of targets and their layout relative to the sensors locations. To identify favorable radars locations with respect to the targets layout, four special cases, demonstrated in Figure 1, are analyzed.

System parameters are set as follows: $\beta_k = 200$ kHz, $\forall k$, $f_c = 2$ GHz (wavelength $\lambda = 1.5$ meter), SNR = 25 dB, and all reflectivity index values are assumed equal $|\zeta^q| = 1$, $\forall q$. Targets are placed in a horizontal shaped structure, with the first target located at $(0, 0)$ and the others located at $(x_q = x_{q-1} + 10, y_q = 0)$.

The averaged value of η_{Spt} versus the number of targets is drawn in Fig. 2. Following the discussion in previous section, we want to avoid $\Delta\tau_{\ell k}^{qq'} \simeq 0$ and keep $\Delta\tau_{\ell k}^{qq'}$ as large as possible. It is observed in the figure that a symmetrical placement, as shown in Case 1, is not an optimal one. Rearranging the radars, in the more favorable setting (as in Case 4) demonstrates a performance gain, in terms of the number of targets and the spatial advantage, achieved without any change in the number of antennas. This is a result of the larger transmit/receive aperture sets contributing to larger delays.

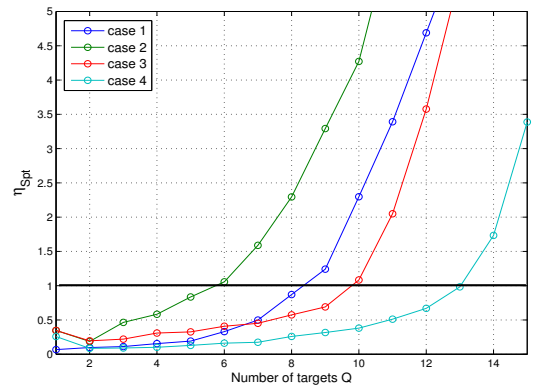

Fig. 2. Spatial advantage values for cases 1 to 4.

Placing the radars in a broadside horizontal spread (as in Case 3) provides better spatial advantage and moderate performance loss rate when compared with Case 2, where a vertical radar setting is used. This is a combined effect of the larger time delays and the impact of matrix $\mathbf{D}$, which provide better horizontal separation in Case 3 [17].

Increasing the number of radars, as can be noticed from comparing cases 3 and 4, allows for localization of more targets with higher spatial advantage and restrained performance loss rate.

V. Conclusions

The analytical expression for the CRLB for the case of multiple targets localization in coherent MIMO radar systems with widely distributed antenna is derived, demonstrating both coherency advantage and spatial advantage. Nonetheless, there is a tradeoff between the ability to localize multiple targets and the accuracy with which it can be done, introduced by the mutual interference between the targets' reflected paths. These cross-correlation terms may be controlled by choosing propitious radars locations. The relation between different sensor schemes and targets layouts on the performance was examined using numerical analysis. It demonstrates the tradeoff between spatial advantage and the number of targets. It is shown that performance loss may be compensated by increasing the number of transmit and/or receive radars or by rearranging the sensors locations. As the CRLB provides a good bound at high SNR, a more rigid bound needs to be found for the low SNR case, where the ambiguities predominate the estimation capabilities.

Appendix I
Derivation of the FIM in (22)

In this appendix, we develop the FIM for the unknown parameter vector ψ, based on the conditional pdf in (9). The block matrices that define $\mathbf{J}(\psi) = E\left\{\nabla_\psi \log p(\mathbf{r}|\psi)\left(\nabla_\psi \log p(\mathbf{r}|\psi)\right)^H\right\} = -E\left[\frac{\partial^2 \log p(\mathbf{r}|\psi)}{\partial^2 \psi}\right]$ are derived hereafter.

The submatrix $\mathbf{\Gamma_x}$, $\mathbf{\Sigma}$, and $\mathbf{V}$ have each the following general form:

$$\mathbf{A} = \begin{bmatrix} \mathbf{A}^{11} & \cdots & \mathbf{A}^{1Q} \\ \vdots & \ddots & \vdots \\ \mathbf{A}^{Q1} & \cdots & \mathbf{A}^{QQ} \end{bmatrix}. \tag{21}$$

The following indexing notations are used throughout: $j = [(\ell-1)*M+k]$; $j' = [(\ell'-1)*M+k']$; $k,k' = 1,..,M$; $\ell,\ell' = 1,..,N$; $q,q' = 1,..,Q$.

Matrix $\mathbf{\Gamma}^{qq'}$ elements are derived as follows:

$$[\mathbf{\Gamma}^{qq'}]_{jj'} = \frac{1}{\eta_o}[\mathbf{J}(\psi)]_{ii'} = -\frac{1}{\eta_o}E\left[\partial^2 \log p(\mathbf{r}|\psi)/\partial\tau^q_{\ell k}\partial\tau^{q'}_{\ell' k'}\right], \tag{22}$$

where $\eta_o = 8\pi^2 \,\mathrm{SNR}\, f_c^2$ and $\log p(\mathbf{r}|\psi)$ is given in (9). In matrix form,

$$\mathbf{\Gamma}^{qq'} = \begin{cases} |\zeta^q|^2 f_{R_k}\mathbf{I}_{MN\times MN} & q=q' \\ \frac{\zeta^q\left(\zeta^{q'}\right)}{\eta_o}\mathrm{Re}\left\{\frac{\partial^2}{\partial\tau^2}\left[\mathbf{\Lambda}^q\mathbf{R}_s^{qq'}\left(\mathbf{\Lambda}^{q'}\right)^H\right]\right\} & q\neq q' \end{cases}, \tag{23}$$

where we define $\mathbf{\Lambda}^q = \mathrm{diag}(\mathbf{e}^q)$. The notation $\mathrm{diag}(\cdot)$ is a diagonal matrix, $\mathbf{e}^q$ is defined as $\mathbf{e}^q = [\exp(-2\pi f_c\tau^q_{11}), \exp(-2\pi f_c\tau^q_{12}), ..., \exp(-2\pi f_c\tau^q_{MN})]^T$, and we abuse the notation and let $\left[\frac{\partial^2}{\partial\tau^2}\mathbf{A}\right]_{jj'} \equiv \frac{\partial}{\partial\tau^q_{\ell k}\partial\tau^{q'}_{\ell' k'}}[\mathbf{A}]_{jj'}$.

The frequency ratio f_{R_k} is defined as $f_{R_k} = \left(1+\beta_k^2/f_c^2\right)$. When we invoke the narrowband assumption $\beta_k^2/f_c^2 \ll 1$ it follows that $f_{R_k} \simeq 1$. The elements of matrix $\mathbf{R}_s$ are defined as:

$$\left[\mathbf{R}_s^{qq'}\right]_{jj'} \equiv \begin{cases} \int s_k(t-\tau^q_{\ell k})\, s_k^*\left(t-\tau^{q'}_{\ell k}\right)dt & \ell=\ell'; k=k' \\ 0 & \ell\neq\ell'; k\neq k' \end{cases} \tag{24}$$

Matrix $\mathbf{\Sigma}$ in (13) is defined by a set of matrices $\mathbf{\Sigma}^{qq'}$ with the following elements:

$$[\mathbf{\Sigma}^{qq'}]_{1,1} = [\mathbf{\Sigma}^{qq'}]_{2,2} = -\frac{1}{\eta_o}E\left[\partial^2 \log p(\mathbf{r}|\psi)/\partial\zeta^q_{re}\partial\zeta^{q'}_{re}\right]$$
$$[\mathbf{\Sigma}^{qq'}]_{1,2} = [\mathbf{\Sigma}^{qq'}]_{2,1} = -\frac{1}{\eta_o}E\left[\partial^2 \log p(\mathbf{r}|\psi)/\partial\zeta^q_{re}\,\partial\zeta^{q'}_{im}\right]. \tag{25}$$

In matrix form,

$$\mathbf{\Sigma}^{qq'} = \begin{cases} \frac{2}{\eta_o}MN\mathbf{I}_{2\times 2} & q=q' \\ \frac{1}{\eta_o}\begin{bmatrix} \mathrm{Re}[\vartheta] & -\mathrm{Im}[\vartheta] \\ -\mathrm{Im}[\vartheta] & \mathrm{Re}[\vartheta] \end{bmatrix} & q\neq q' \end{cases}, \tag{26}$$

where we use the notation $\vartheta = (\mathbf{e}^q)^T\mathbf{R}_s^{qq'}\left(\mathbf{e}^{q'}\right)^*$.

Matrix $\mathbf{V}$ in (13) is defined by set of matrices $\mathbf{V}^{qq'}$ with the following elements:

$$[\mathbf{V}^{qq'}]_{i1} = -\frac{1}{\eta_o}E\left[\partial^2 \log p(\mathbf{r}|\psi)/\partial\tau^q_{\ell k}\,\partial\zeta^{q'}_{re}\right] \tag{27}$$
$$[\mathbf{V}^{qq'}]_{i2} = -\frac{1}{\eta_o}E\left[\partial^2 \log p(\mathbf{r}|\psi)/\partial\tau^q_{\ell k}\,\partial\zeta^{q'}_{im}\right], \tag{28}$$

In matrix form,

$$\mathbf{V}^{qq'} = \begin{cases} \sqrt{\frac{2}{\eta_o}}\begin{bmatrix} -\zeta^q_{im} \\ \zeta^q_{re} \end{bmatrix} & q=q' \\ \frac{1}{\eta_o}\begin{bmatrix} \mathrm{Re}\left\{\zeta\frac{\partial}{\partial\tau}\left[\mathbf{\Lambda}^q\mathbf{R}_s\left(\mathbf{e}^{q'}\right)^*\right]\right\} \\ -\mathrm{Im}\left\{\zeta\frac{\partial}{\partial\tau}\left[\mathbf{\Lambda}^q\mathbf{R}_s\left(\mathbf{e}^{q'}\right)^*\right]\right\} \end{bmatrix} & q\neq q' \end{cases}. \tag{29}$$

Acknowledgement 1: The authors would like to acknowledge helpful discussions with Dr. J. L. Krolik of Duke University.

References

[1] E. Fishler, A. M. Haimovich, R. S. Blum, L. Cimini, D. Chizhik, and R. Valenzuela, "MIMO radar: an idea whose time has come," in *Proc. of the 2004 IEEE Int. Conf. on Radar*, April 2004, pp. 71–78.

[2] A. Haimovich, R. Blum, L. Cimini, , "MIMO Radar with Widely Separated antennas", *IEEE Signal Proc. Magazine*, January 2008.

[3] H. Godrich, A.M Haimovich, and R.S. Blum, "*Concepts And Applications Of MIMO Radar Sysem With Widely Separated Antenna.,*" Book Chapter, 2009.

[4] J. Li, and P. Stoica, "MIMO Radar with Colocated antennas", *IEEE Signal Proc. Magazine*, September 2007, pp. 106–114.

[5] F. C. Robey, S. Coutts, D. Weikle, J. C. McHarg, and K. Cuomo, "MIMO radar theory and experimental results," in *Proc. of 37th ASILOMAR 2004 Conf. on Signals, Systems and Computers*, Nov. 2004, pp. 300–304.

[6] L. Xu, J. Li, P. Stoica, K.W. Forsythe, and D.W. Bliss, "Waveform optimization for MIMO radar: A Cramer-Rao bound based study," in Proc. 2007 IEEE Int. Conf. Acoustics, Speech, and Signal Processing, Honolulu, Hawaii, pp. II-917–11-920, April 2007.

[7] D. R. Fuhrman, and G. San Antonio, "Transmit beam-forming for MIMO radar systems using partial signal correlation," in *Proc. of 38th ASILOMAR 2004 Conf. on Signals, Systems and Computers*, Nov. 2004, pp. 295–299.

[8] D. W. Bliss, and K. W. Forsythe, "Multiple-input multiple-output (MIMO) radar and imaging: degrees of freedom and resolution," in *Proc. of 37th ASILOMAR 2003 Conf. on Signals, Systems and Computers*, Nov. 2003, pp. 54–59.

[9] I. Bekkerman and J. Tabrikian, "Target detection and localization using MIMO radars and sonars," *IEEE Trans. on Sig. Proc.*, vol. 54, pp. 3873–3883, Oct. 2006.

[10] J. Li, P. Stoica, L. Xu, and W. Roberts, "On parameter identifiability of MIMO radar," *IEEE Signal Processing Lett.*, vol. 14, no. 12, Dec. 2007.

[11] N. Lehmann, A. M. Haimovich, R. S. Blum, and L. Cimini, "High resolution capabilities of MIMO radar," in *Proc. of 40th ASILOMAR 2006 Conf. on Signals, Systems and Computers*, Nov. 2006.

[12] H. Godrich, A. M. Haimovich, and R. S. Blum, "Cramer Rao Bound on Target Localization Estimation in MIMO Radar Systems", in *Proc. of CISS Conf.*, March 2008.

[13] H. Godrich, A. M. Haimovich, and R. S. Blum, "Target localization accuracy gain in MIMO radar based system," submitted to *IEEE Trans. on Information Theory.*

[14] M. A. Haleem and A. Haimovich, "On the distribution of ambiguity levels in MIMO radar," in *Proc. of 42nd ASILOMAR 2008 Conf. on Signals, Systems, and Computers,* Nov. 2008.

[15] S. M. Kay, *Fundementals of Statistical Signal Processing: Estimation Theory,* vol. 1, New Jersey: Parentice Hall PTR, 1st ed., 1993.

[16] M. Skolnik, *Introduction to Radar Systems*. New York: McGraw-Hill, 3rd, 2002.

[17] M. Hamilton and P. M. Schultheiss, "Passive Ranging in Mulyipath Dominant Environment, Part I: Known Multipath Parameters," in *IEEE. trans on Signal Proc.* vol. 40, no. 1, Jan. 1992.